INVENTORY OF SUPPLEMENTAL INFORMATION

Supplemental Information includes two tables, five figures, and detailed experimental procedures. The first table lists all significant and suggestive QTLs for Figure 4C and the second lists full correlation details for Figure 6B. The five figures show additional correlations and comparisons tangential to Figures 1, 4, 5, 6, and 7 as outlined in the main text of the paper. The supplemental experimental procedures provide a detailed description of the phenotyping procedures and bioinformatic analyses. All phenotype data can be found with the article online as well as on the GeneNetwork resource (change "Type" to "Phenotypes" and search "Get Any:" for "LISP1").

SUPPLEMENTAL INFORMATION

Systems genetics of metabolism - the use of the BXD murine reference panel for multiscalar integration

Pénélope A. Andreux[1†], Evan G. Williams[1†], Hana Koutnikova[2$], Riekelt H. Houtkooper[1$], Marie-France Champy[2], Hugues Henry[3], Kristina Schoonjans[1], Robert W. Williams[4], Johan Auwerx[1,2]

Supplementary data

Figure S1

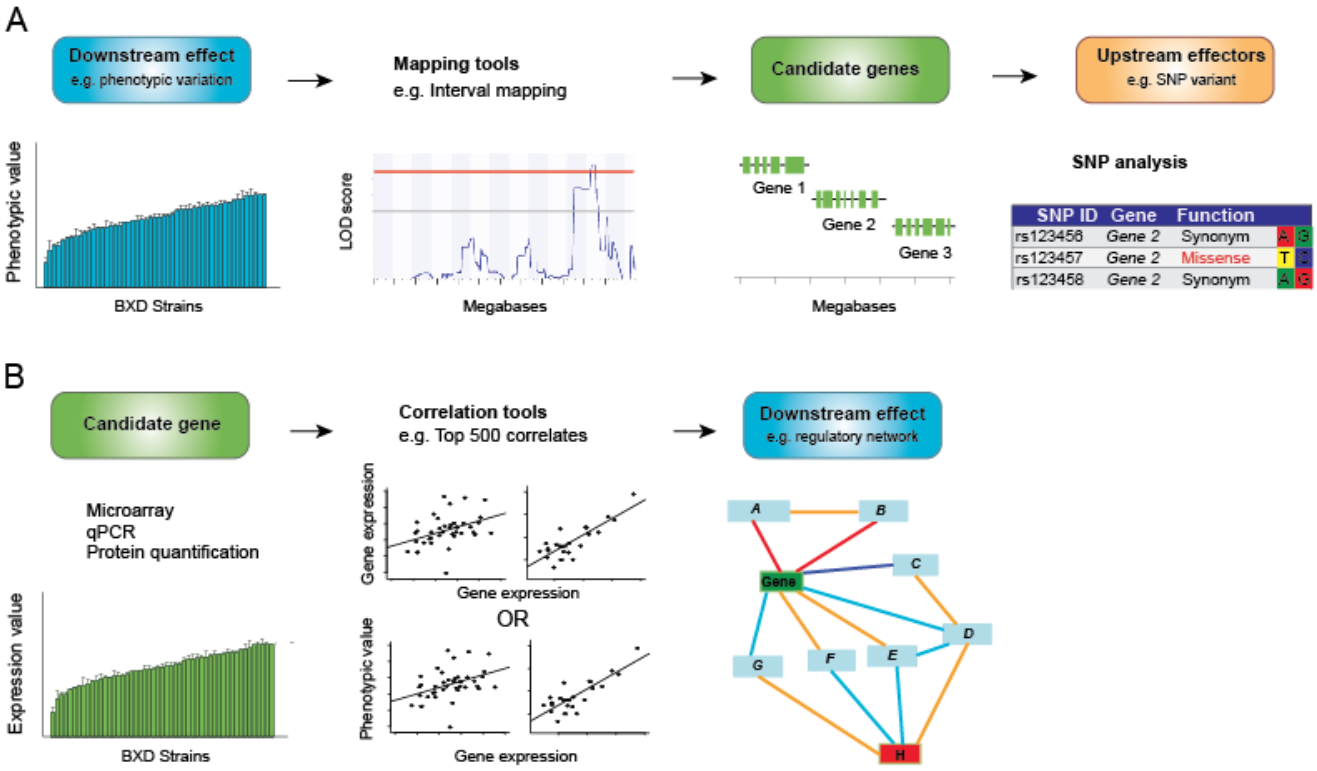

Figure S1. Process Paths for Forward and Reverse Genetics Approaches. Related to Figure 1

(A) The forward genetics approach. Starting from downstream effects such as variation in phenotype, QTL mapping allows for the identification of candidates, which can then be further narrowed down to upstream effectors such as SNPs. Two examples of this approach are given in Figures 4 and 5. (B) The reverse genetics approach. Starting from expression data of a gene of interest, correlation analysis with expression data of other genes or phenotypic data allows the creation of a network and the identification of downstream effects. Detailed examples of this approach are given in Figures 6 and 7.

Figure S2

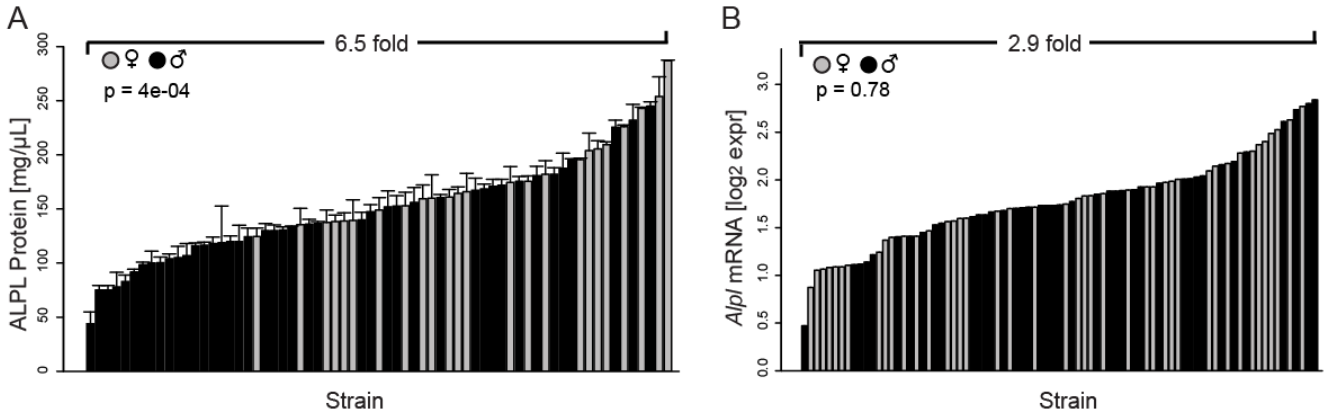

C

SNP ID	Chr	Mb	Domain	Function	B	D
rs27576148	4	137.298457	Exon 12	Synonym	A	G
rs27576144	4	137.299107	Exon 11	Synonym	T	C
rs13471138	4	137.299134	Exon 11	Synonym	G	A
rs27576142	4	137.299173	Exon 11	Synonym	G	A
rs31936070	4	137.302334	Exon 9	MISSENSE	A	G
wt37-4-137302352	4	137.302352	Exon 9	MISSENSE	C	T
rs27576112	4	137.305509	Exon 7	Synonym	G	A
rs27576111	4	137.305557	Exon 7	Synonym	A	G
rs27576110	4	137.305560	Exon 7	Synonym	A	G
wt-4-137309862	4	137.309862	Exon 5	Synonym	G	A
wt-4-137309931	4	137.309931	Exon 5	Synonym	A	G

Figure S2. ALPL Comparison between male and female animals. Related to Figure 4.

(A) Females have significantly higher levels of ALPL protein in the blood than males (180±8.8 mg/µL vs. 138±6.8 mg/µL, *p* = 4e-4). This comparison holds true when strains are separated by allele: females with the B allele average 157±4.8 mg/µL while males with the B allele have 112±5.4 mg/µL (*p* = 3.2e-8); females with the D allele have 233±11.6 mg/µL and males 176±8.6 mg/µL (*p* = 2e-7). (B) Although mRNA expression of *Alpl* in the liver was not significantly different between males and females, strains with the D allele had significantly higher *Alpl* expression than strains with the B allele (*p* = 6.2e-6). (C) List of SNPs between DBA/2 and C57BL/6 in the exons of *Alpl*. The two missense mutations that result in the amino acid changes R318Q and L324P are noted.

Figure S3.

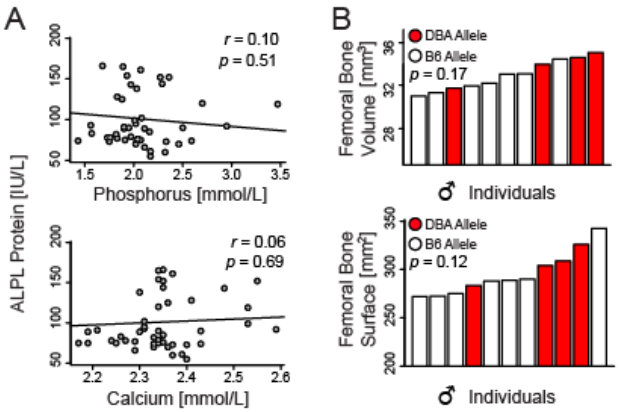

Figure S3. Links to Hypophosphatasia. Related to Figure 5.

(A) ALPL levels do not correlate with phosphorus or calcium. Together with the strong correlation between PLP and ALPL, these data indicate hypophosphatasia and contraindicate other potential diseases. (B) Analysis of male femurs also shows a tendency for decreased bone surface/volume in animals with the B allele of *Alpl*. Male femurs are significantly more voluminous and larger in surface area than females ($p < 0.05$, $p < 0.001$).

Figure S4

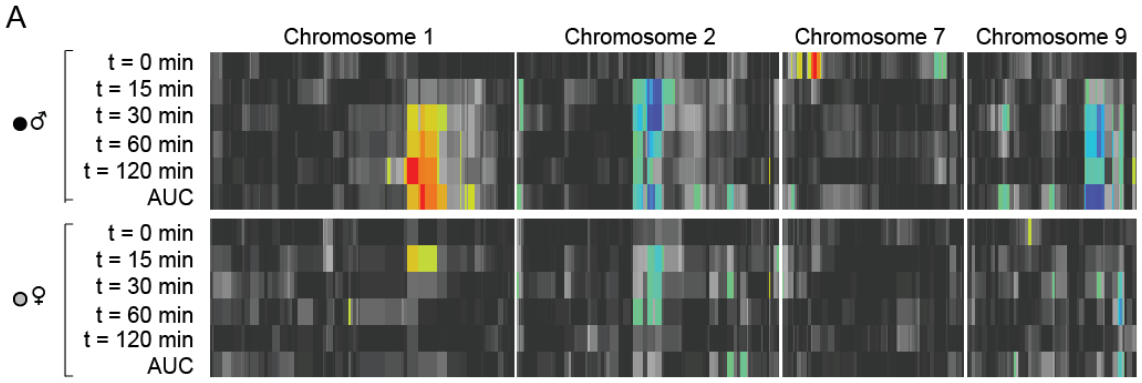

Figure S4. Multiple heatmap for male and female glucose tolerance traits on chromosomes 1, 2, 7 and 9. Related to Figure 6.

Males and females present common and distinct QTLs. Only the glucose level at 15 minutes in females aligns with the QTL on Chr1 that is observed in males. For Chr2, glucose at 15, 30 and 60 minutes in females map on the same QTLs as the males. The QTLs on Chr7 and 9 are male-specific. The LRS values of the QTLs in females are considerably lower compared to males, partly due to the lower number of strains. No other significant QTLs were observed for the glucose tolerance in females on the rest of the genome.

Figure S5.

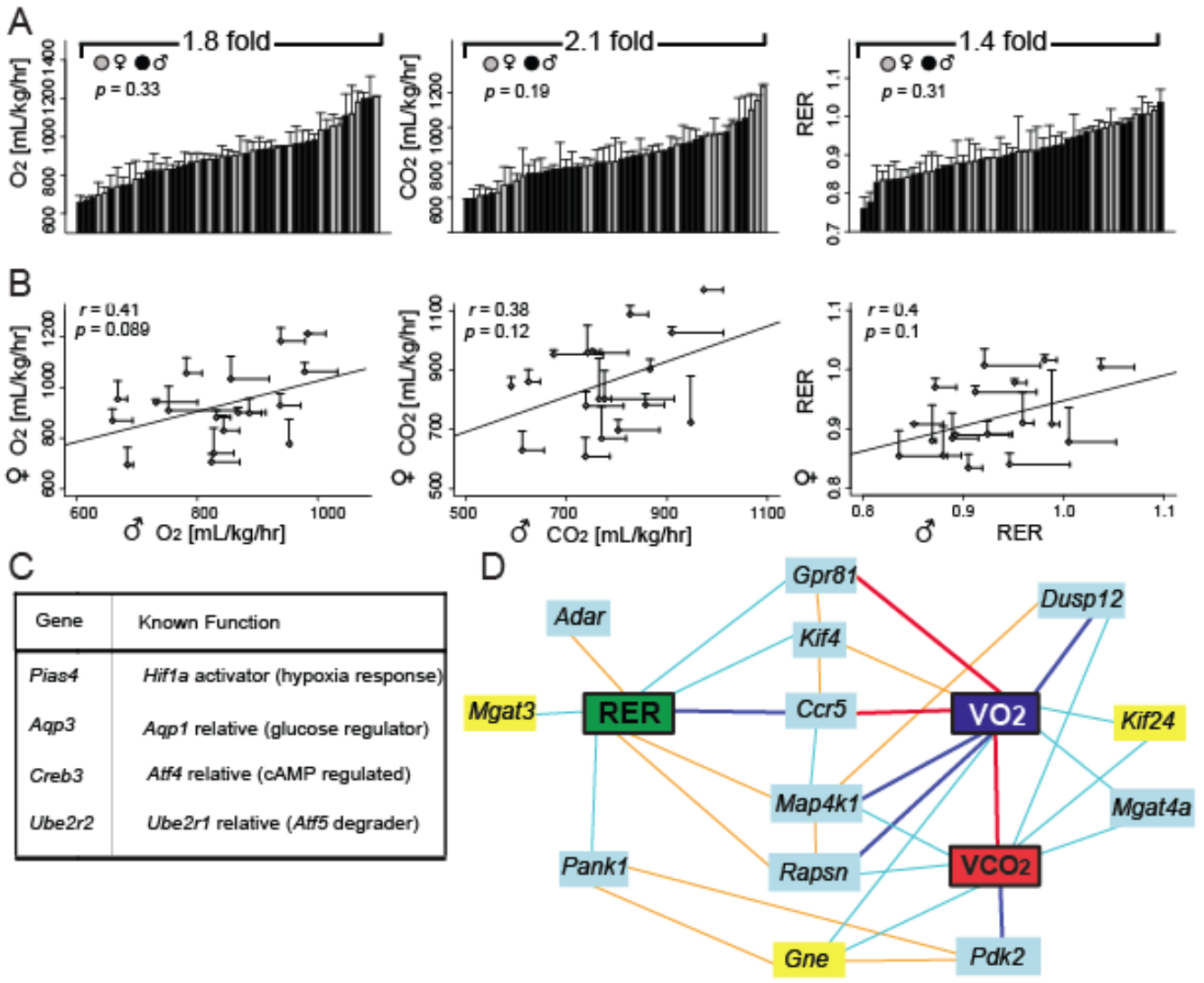

Figure S5. Energy expenditure parameters. Related to Figure 7.

(A) No significant differences were observed between male and female animals in any of the measured parameters. (B) Suggestive, but non-significant, correlations were observed when the parameters from each sex were correlated by strain (panel B). (C) Network analysis of energy regulation of the eye network in Figure 7D also revealed tightly covarying positional candidates with no known, direct link to the phenotype. However, these genes—*Pias4*, *Aqp3*, *Creb3,* and *Ube2r2*—belong to or modulate gene families that are important for respiration. *Pias4* modulates hypoxia response by inhibiting hypoxia-inducible factor 1 alpha and thereby affects anaerobic metabolism (Kang et al., 2010). *Creb3* has no established links to energy metabolism, but belongs to the same

family as *Atf4*. Similarly, *Aqp1* acts on glucose regulation via the IGF1 pathway in worms (Lee et al., 2009), and *Ube2r1* mediates degradation of *Atf5* (Wei et al., 2008). (D) A network analysis was generated using techniques identical to that used for Figure 7D but instead using the same liver dataset used for the glucose network (Gatti et al., 2007). The top mRNA correlate network (again including positional candidates in yellow) reveals many common candidates (e.g. *Pank1*, *Adar*, *Kif4*) as well as some new potential candidates; e.g. chemokine receptor 5, *Ccr5*, is centrally located and potentially a significant regulator of oxidative metabolism due to its regulation of airway inflammation (Fuchimoto et al., 2011).

Table S1. List of QTLs for traits with significant or suggestive peaks. Related to Figure 4.

Trait Description	LOD	p-val	Chr@Mb*
Alkaline Phosphatase Levels (♂)	6.8	1.6e-5	Chr4@131.5
Alkaline Phosphatase Levels (♀)	6.6	2.3e-5	Chr4@139.3
Blood Cell Volume (♂)	6.1	7.3e-5	Chr7@114.5
Blood Cell Volume (♀)	5.5	3.3e-4	Chr7@114.5
White Blood Cell Count (♀)	5.5	3.3e-4	Chr10@120.1
Hemoglobin Concentration (♂)	5.1	8.0e-4	Chr7@111.3
Hemoglobin Concentration (♀)	4.0	9.2e-3	Chr7@114.5
CO2 Production (♂)	4.8	1.7e-3	Chr1@57.9
Hematocrit (♂)	4.8	3.1e-3	Chr7@114.5
Systolic Blood Pressure (♂)	4.7†	3.2e-3	Chr9@113.2
Heart Rate (♀)	4.5	3.7e-3	Chr19@33.0
Bone Surface Area (♀)	4.4	3.8e-3	Chr13@71.1
Fasting Glucose (♀)	4.3	5.1e-3	Chr6@149.0
RER (♀)	4.3	5.6e-3	Chr9@83.6
IPGTT Glucose Response (♂)	4.1	7.2e-3	Chr9@103.8
White Blood Cell Count (♂)	4.1	7.6e-3	Chr3@28.3
Bone Surface Area (♂)	4.1	7.6e-3	Chr5@74.2
Phosphorus Levels (♂)	4.0	9.2e-3	Chr17@65.3
Left Ventricular Mass (♀)	4.0	.010	Chr15@32.6
Body Weight (18 weeks old) (♀)	3.9	.011	Chr16@69.8
Platelet Count (♀)	3.9	.011	Chr13@100.1
ALAT Levels (♀)	3.8	.018	Chr13@90.4
IPGTT Response AUC (♂)	3.7	.020	Chr9@103.8
HBB Level (♂)	3.6	.023	Chr7@118.8
VO2 Production (♂)	3.6	.023	Chr1@55.2
Triglyceride Levels (♂)	3.6	.023	Chr7@31.5
Body Weight (17 weeks) (♀)	3.6	.023	Chr6@149.0
Albumin Levels (♀)	3.6	.023	Chr16@56.5
Phosphorus Levels (♀)	3.6	.024	Chr3@84.9
RER (♂)	3.6	.024	Chr10@118.9
IPGTT Glucose @ 30 min (♂)	3.6	.028	Chr2@98.0
Body Weight (20 weeks) (♀)	3.5	.029	Chr17@74.2
ALAT Levels (♂)	3.5	.032	Chr1@154.4
Water Intake (♀)	3.4	.036	Chr13@13.8
Shortening Fraction (♂)	3.4	.036	Chr17@70.6
Creatinine Levels (♀)	3.4	.039	Chr6@8.4
Body Weight (18 Weeks) (♂)	3.4	.039	Chr2@98.0
Bone Mineral Content (♀)	3.4	.039	Chr13@71.1
Heart Rate (♂)	3.4	.043	Chr19@37.8
Lean Mass Percent (♂)	3.3	.053	ChrX@147.8
Fasting Glucose Levels (♂)	3.3	.053	Chr7@48.2

Bone Mineral Density (♂)	3.3	.053	Chr17@72.6
IPGTT Response AUC (♀)	3.3	.056	Chr4@155.4
Albumin Levels (♂)	3.2	.065	Chr4@32.2
Lean Mass Weight (♀)	3.1	.072	Chr3@57.6
Cholesterol Levels (♀)	3.1	.072	Chr3@35.5
Food Intake (♀)	3.1	.075	Chr13@99.6
IPGTT Glucose @ 120 min (♂)	3.1	.087	Chr1@147.4
Ejection Fraction (♂)	3.1	.087	Chr6@136.7
Bone Mineral Content (♂)	3.0	.092	Chr16@24.2
Blood Protein (Total) (♂)	3.0	.097	Chr4@32.2
Sodium Levels (♀)	3.0	.097	Chr3@90.4
Septum Thickness (♂)	3.0	.097	Chr10@17.7
Body Weight (17 Weeks) (♂)	3.0	.097	Chr9@47.4

Table S2. Correlation of glucose tolerance and body weight parameters in males and females. Related to Figure 6.

A

Males / **Females**	White adipose tissue mass (g)	Lean mass (g)	Body weight (g)	OGTT AUC
OGTT AUC	0.064 p = 0.773	0.292 p = 0.179	-0.019 p = 0.933	**0.543** **p = 6.51E-03**
Body weight (g)	0.220 p = 0.317	0.218 p = 0.321	0.335 p = 0.119	
Lean mass (g)	-0.205 p = 0.351	**0.695** **p = 1.27E-04**		
White adipose tissue mass (g)	0.392 p = 0.063			

B

Males	White adipose tissue mass (g)	Lean mass (g)	Body weight (g)	OGTT AUC
OGTT AUC	**0.513** **p = 4.79E-04**	0.226 p = 0.151	0.280 p = 0.072	
Body weight (g)	**0.544** **p = 1.68E-04**	**0.789** **p = 2.48E-11**		
Lean mass (g)	0.230 p = 0.149			
White adipose tissue mass (g)				

C

Females	White adipose tissue mass (g)	Lean mass (g)	Body weight (g)	OGTT AUC
OGTT AUC	0.153 p = 0.480	-0.120 p = 0.581	-0.1 p = 0.646	
Body weight (g)	**0.615** **p = 0.001**	**0.504** **p = 0.011**		
Lean mass (g)	-0.047 p = 0.830			
White adipose tissue mass (g)				

SUPPLEMENTAL EXPERIMENTAL PROCEDURES

Clinical Phenotyping Tests

Detailed procedures are found on EMPReSS (empress.har.mrc.ac.uk/browser/) and are described in (Champy et al., 2004; Champy et al., 2008). In brief, energy expenditure was measured by indirect calorimetry in Oxymax metabolic cages (Columbus Instruments). Blood pressure was measured using a tail-cuff system, the BP-2000 Blood Pressure Analysis System (Visitech Systems) (Koutnikova et al., 2009). Cardiac function was assessed by echocardiography on anesthetized animals using a HP Sonos 5500 with a 15MHz linear transducer (Philips Healthcare). Glucose tolerance was analyzed by measuring blood glucose and insulin following intra-peritoneal injection (glucose 2g/kg of mouse) after an overnight fast (Heikkinen et al., 2007). Body composition and bone density were determined using a DEXA-scan Lunar PIXImus Densitometer (GE Medical Systems). At sacrifice, blood and tissues including the heart, liver, kidney, gastrocnemius, soleus and adipose deposits were weighed and collected. Hematology analysis were performed on fresh blood with a Ac•T diff analyzer (Beckman Coulter). Clinical parameters were measured in plasma using an AU400 immuno analyzer (Olympus). Animals from the 11 strains used for supplemental phenotyping on ALPL ranged in age from 40 to 52 weeks. Ages were balanced between animals with each allele of ALPL. Pyridoxal and pyridoxal-phosphate were measured by HPLC using a commercial assay (Vitamin B6 in plasma, Recipe).

Bone Scan Parameters

A SkyScan 1076 In-vivo X-ray Micro-CT (SkyScan) was used for all femur CT analyses. The source power was maximized at 80 kV and 120 µA. An aluminum filter of 0.5mm was used. The scans were performed with 180° rotations at 9 µm resolution with a rotation step of 0.8 degrees. Exposure of 1600 ms with a HU calibration of 16000 was used for each slice. The accompanying CTAn software (SkyScan) was used for all bone analyses. 3D reconstructions were created after a histogram cutoff of 0–50 units assigned to tissue and 50–255 for bone.

Bioinformatics and Statistical Analysis Detail

GeneNetwork contains a comprehensive database of microarray data for the BXDs along with thousands of phenotypes and sequence and genotype information which were used to supplement findings from this resource data. All genetic positions are given according to data from the Build 37 *Mus musculus* genome assembly from NCBI and the Mouse Genome Sequencing Consortium (MGSCv37). Power calculations were performed using the R/qtlDesign package. Environmental variance was set to 40 units and genetic variance set at 60 units (i.e. h^2 of 0.60); these variance values were estimated on previous phenotypic measurements from the BXDs (Chesler et al., 2004). Power estimates were later confirmed by calculating the heritability of the metabolic traits outlined in this study. Some historical BXD data were used to supplement analysis in this metabolic resource when indicated in the paper. *P*-values of 0.05 and 0.1 were considered the significant and suggestive thresholds for male vs. female comparisons and for *X*-*Y* correlation plots. LOD scores of 3.3 and 3.0 were considered the significant and suggestive thresholds for genetic mapping, where LOD ~ -log(*p*). The associated *p*-values displayed take multiple testing into account—roughly 100 linkage events per strain. CLUSTAL and Genious were used to compare ALPL sequence via BLAST across species and to generate the phylogenic tree.

Design of Network Graphs

The network graphs in Figures 6D, 7C/D, and S4C were hand-drawn from correlation matrices generated from candidate genes and the phenotypes. Genes with median (across the BXDs) expression below the noise threshold were removed prior to analysis. Network graphs used cutoff thresholds of Pearson's *r* of ±0.7 and ±0.5 with varying significance depending on the figure. Pearson's *r* was used as the cutoff for drawing edges rather than a *p* value in order to keep consistency across the three network graphs and due to differing significances for a given *r* within a single network graph (gene to gene correlations have higher *n* than gene to phenotype correlations). For Figure 6D, $r = \pm 0.5$ between genes and the phenotype corresponds to a nominal $p \sim 0.03$ ($n = 18$), and nominal $p \sim 0.0006$ ($n = 41$) between two genes. For Figure 7D, $r = \pm 0.5$ between phenotypes and

genes corresponds to $p \sim 0.008$ ($n = 26$) and $p \sim 0.000005$ ($n = 72$) between two genes. For Figure S4C, $r = \pm 0.5$ between phenotypes and genes corresponds to $p \sim 0.08$ ($n = 13$) and $p \sim 0.0006$ between two genes ($n = 41$).

Selection of QTL Candidate Genes

For the top 10 distinct QTLs listed in Figure 4, all positional candidates in the significant region of the QTL were selected for further analysis. A system was applied, where candidates were favored based on five criteria: 1) exact LOD score at the gene location, 2) mRNA correlation in relevant tissues, when applicable, 3) presence and strength of *cis*-QTLs, 4) presence of and suspected impact from sequence variants, and 5) literature correlation score, calculated using the Semantic Gene Organizer software (Homayouni et al., 2005). In some instances (e.g. alkaline phosphatase levels and mean red blood cell volume) a single gene came out as by far the strongest candidate (*Alpl* and *Hbb* respectively). In other cases, the gene listed in Figure 4 is what we viewed as the strongest candidate, but others potential candidates remain.

SUPPLEMENTAL REFERENCES

Fuchimoto, Y., Kanehiro, A., Miyahara, N., Koga, H., Ikeda, G., Waseda, K., Tanimoto, Y., Ueha, S., Kataoka, M., Gelfand, E.W.*, et al.* (2011). Requirement for chemokine receptor 5 in the development of allergen-induced airway hyperresponsiveness and inflammation. American journal of respiratory cell and molecular biology *45*, 1248-1255.

Heikkinen, S., Argmann, C.A., Champy, M.F., and Auwerx, J. (2007). Evaluation of glucose homeostasis. Curr Protoc Mol Biol *Chapter 29*, Unit 29B 23.

Homayouni, R., Heinrich, K., Wei, L., and Berry, M.W. (2005). Gene clustering by latent semantic indexing of MEDLINE abstracts. Bioinformatics *21*, 104-115.

Kang, X., Li, J., Zou, Y., Yi, J., Zhang, H., Cao, M., Yeh, E.T., and Cheng, J. (2010). PIASy stimulates HIF1alpha SUMOylation and negatively regulates HIF1alpha activity in response to hypoxia. Oncogene *29*, 5568-5578.

Lee, S.J., Murphy, C.T., and Kenyon, C. (2009). Glucose shortens the life span of C. elegans by downregulating DAF-16/FOXO activity and aquaporin gene expression. Cell Metab *10*, 379-391.

Wei, Y., Jiang, J., Liu, D., Zhou, J., Chen, X., Zhang, S., Zong, H., Yun, X., and Gu, J. (2008). Cdc34-mediated degradation of ATF5 is blocked by cisplatin. J Biol Chem *283*, 18773-18781.

FigureS1-RelatedtoFig1

Click here to download Supplemental Figure: FigureS1-GeneticAnalysisProcess.eps

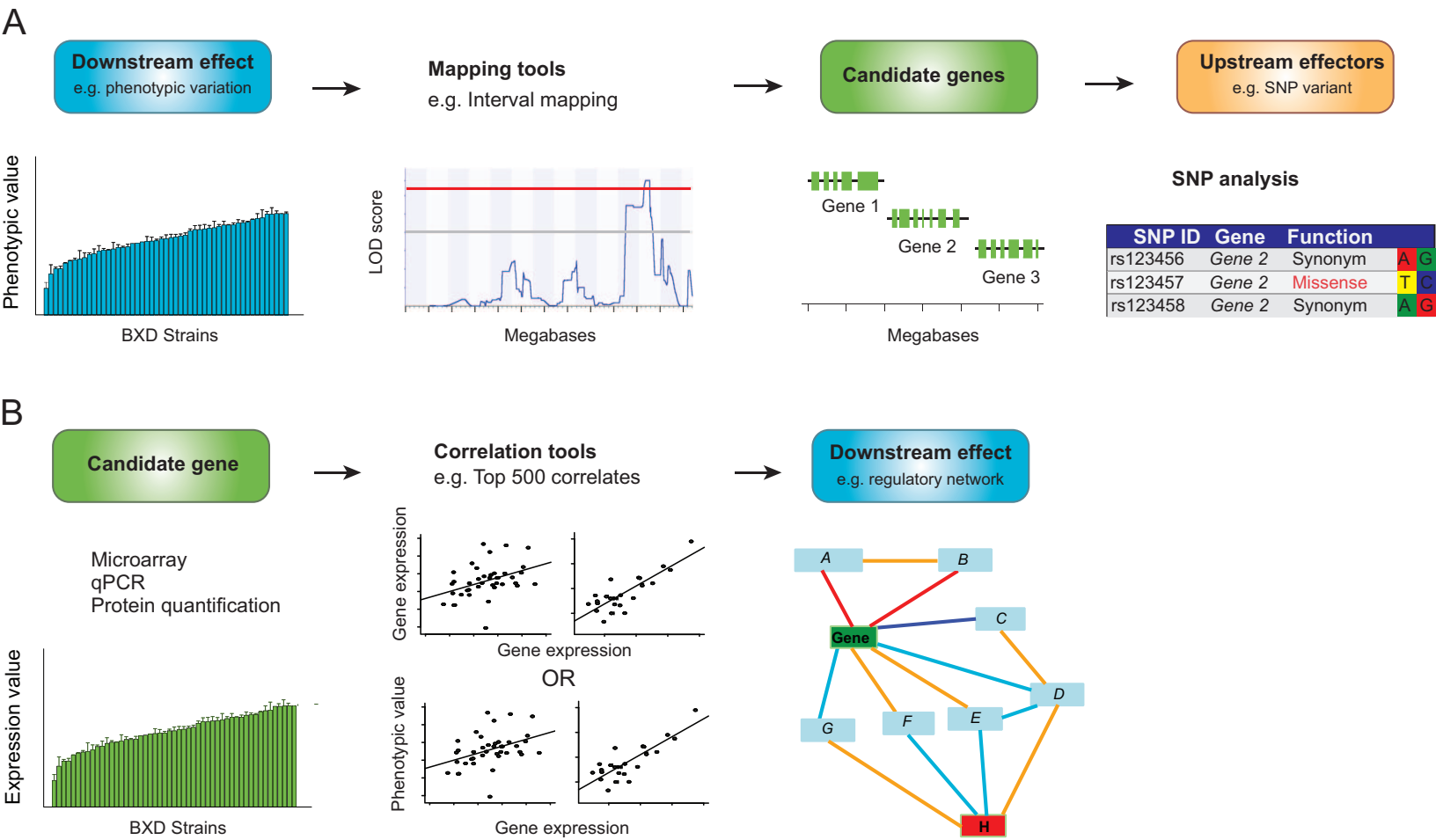

FigureS2-RelatedtoFig4

Click here to download Supplemental Figure: FigureS2-ALPL_Sexes.eps

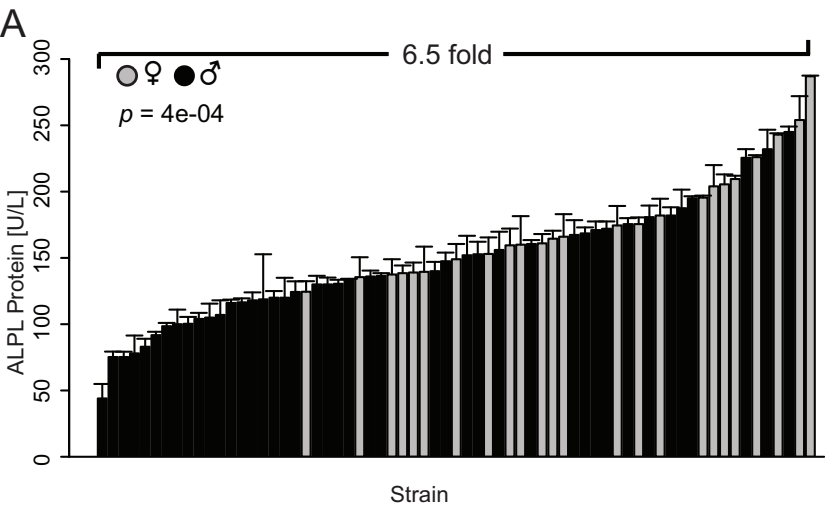

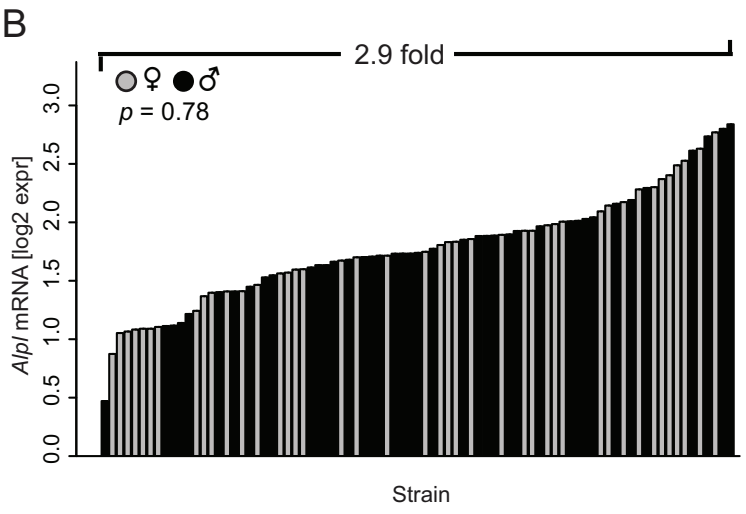

C

Exonic SNPS in region of *Alpl*

SNP ID	Chr	Mb	Domain	Function	B	D
rs27576148	4	137.298457	Exon 12	Synonym	A	G
rs27576144	4	137.299107	Exon 11	Synonym	T	C
rs13471138	4	137.299134	Exon 11	Synonym	G	A
rs27576142	4	137.299173	Exon 11	Synonym	G	A
rs31936070	4	137.302334	Exon 9	MISSENSE	A	G
wt37-4-137302352	4	137.302352	Exon 9	MISSENSE	C	T
rs27576112	4	137.305509	Exon 7	Synonym	G	A
rs27576111	4	137.305557	Exon 7	Synonym	A	G
rs27576110	4	137.305560	Exon 7	Synonym	A	G
wt-4-137309862	4	137.309862	Exon 5	Synonym	G	A
wt-4-137309931	4	137.309931	Exon 5	Synonym	A	G

FigureS3-RelatedtoFig5

Click here to download Supplemental Figure: FigureS3-ALPL_Male_Repheno.eps

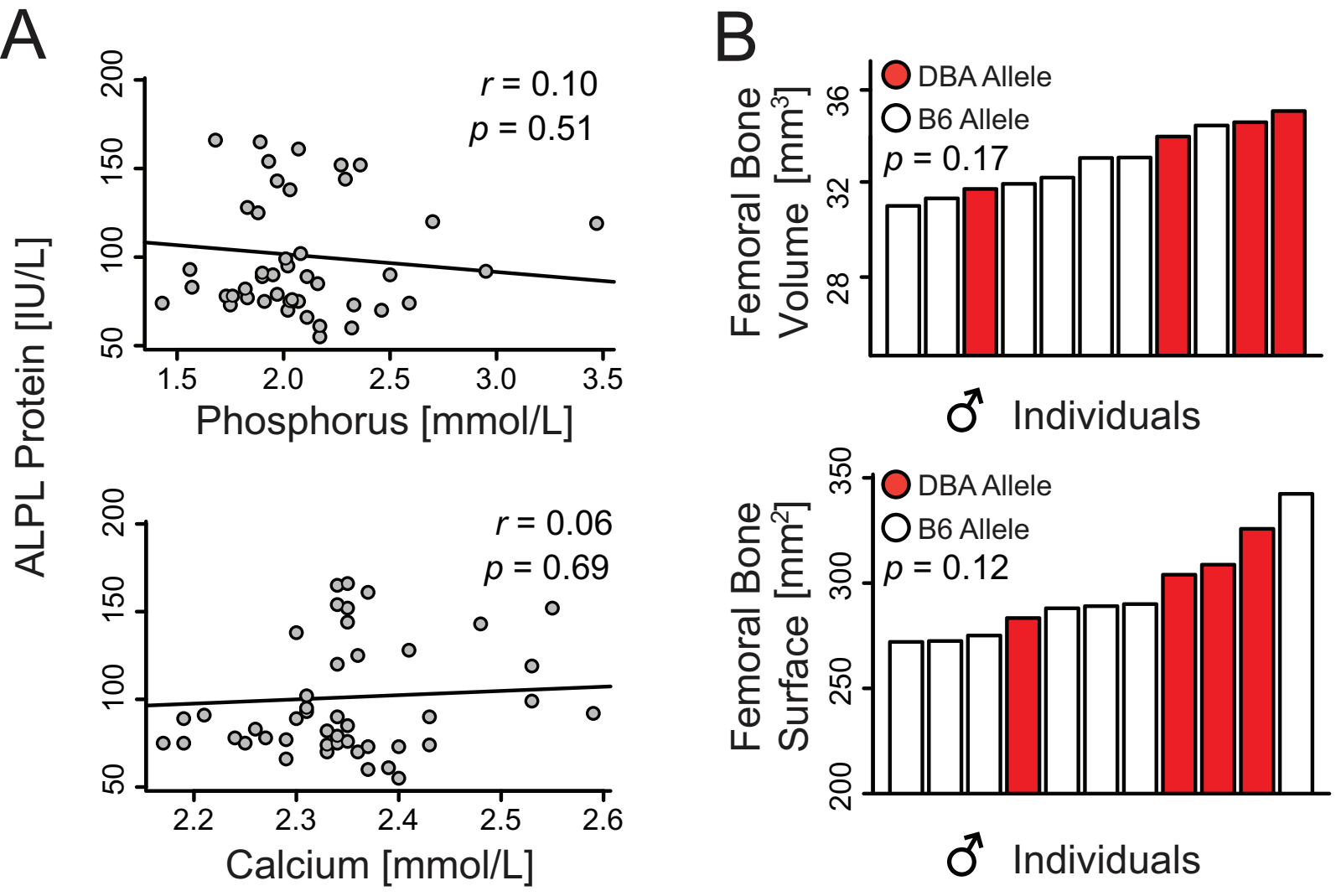

FigureS4-RelatedtoFig6

Click here to download Supplemental Figure: FigureS4-IPGTT M vs F Heatmap.eps

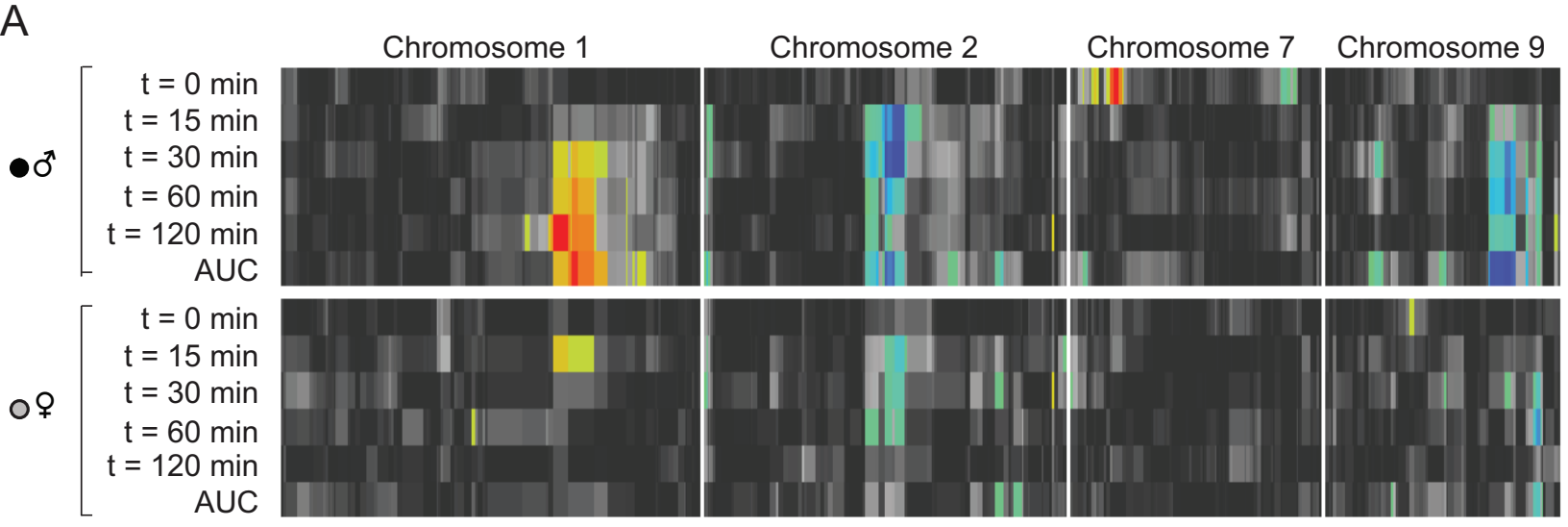

FigureS5-RelatedtoFig7

Click here to download Supplemental Figure: FigureS5-Respiration M vs F.eps

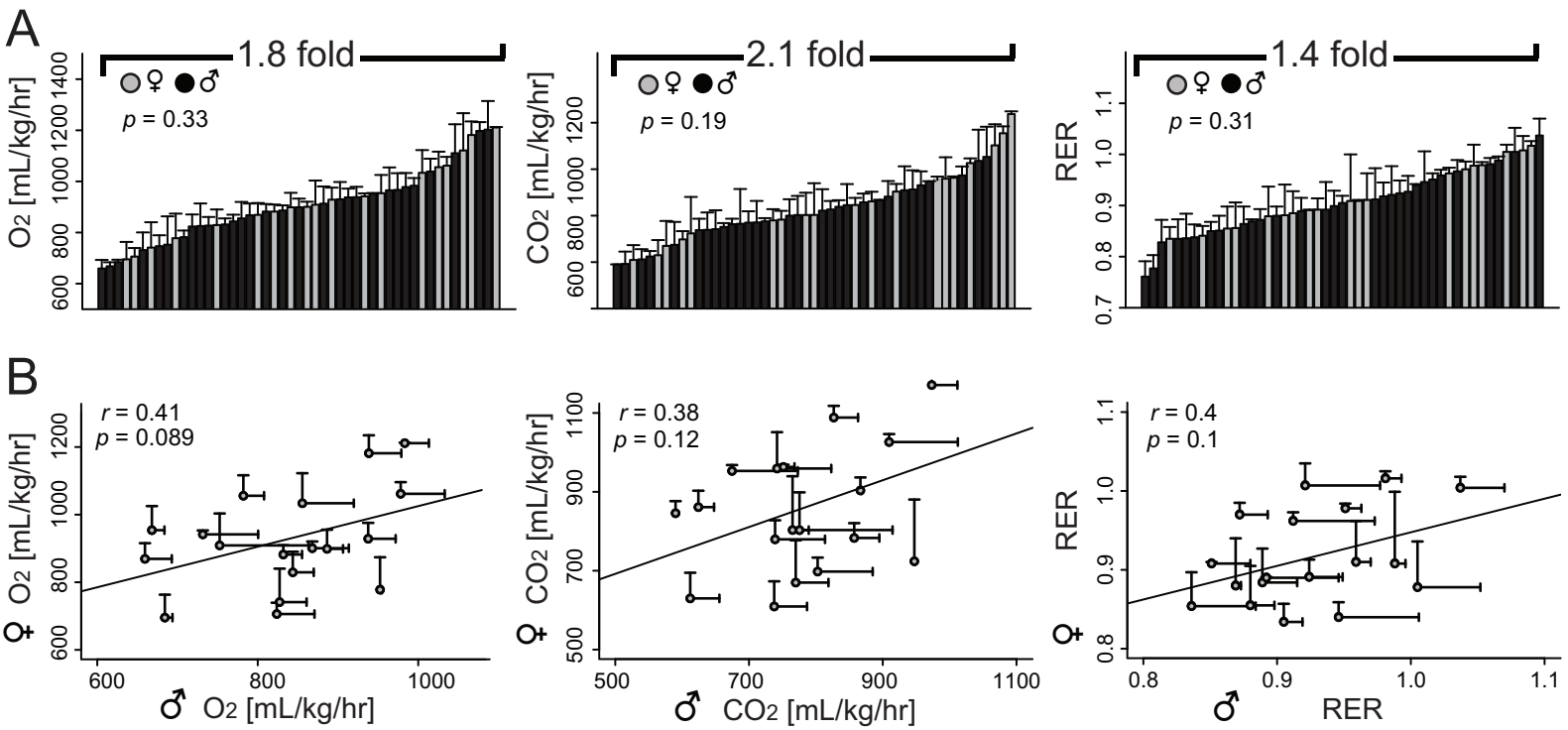

C

Gene	Known Function
Pias4	*Hif1a* activator (hypoxia response)
Aqp3	*Aqp1* relative (glucose regulator)
Creb3	*Atf4* relative (cAMP regulated)
Ube2r2	*Ube2r1* relative (*Atf5* degrader)